

Incompressibility of polydisperse random close packed colloidal particles

Rei Kurita¹ and Eric R. Weeks²

¹*Institute of Industrial Science, The University of Tokyo,
4-6-1 Komaba, Meguro-ku, Tokyo 153-8505, Japan*

²*Department of Physics, Emory University, Atlanta, Georgia 30322, USA*
(Dated: July 17, 2018)

We use confocal microscopy to study a random close packed sample of colloidal particles. We introduce an algorithm to estimate the size of each particle. Taking into account their sizes, we compute the compressibility of the sample as a function of wave vector q , and find that this compressibility vanishes linearly as $q \rightarrow 0$. The particle sizes must be considered to calculate the compressibility properly. These results also suggest that the experimental packing is hyperuniform.

PACS numbers: 82.70.-y, 61.20.-p, 64.70.pv, 64.70.kj

The random packing of objects has been studied scientifically for nearly a century [1, 2]; see Ref. [3] for a review. This problem is often termed “random close packing” (rcp) or “maximally random jammed packing” [4]. Important recent work has focused on the packing of highly polydisperse systems [5], ellipsoids [6], and tetrahedra [7], but the simplest packing problem is the packing of monodisperse spheres. In the past decade, simulations studying monodisperse spheres have generated large rcp configurations with $10^5 - 10^6$ spheres [8, 9]. These simulations enable study of density fluctuations at very large length scales, or equivalently, small wave vectors q . They find that the static structure factor $S(q)$ approaches zero linearly as $q \rightarrow 0$, that is, $S(q) \sim q$ for small q . This finding has been termed “hyperuniformity” [8]. One corollary is that the sample is incompressible, as the isothermal compressibility χ in simple liquids can be found from $\rho k_B T \chi = S(0)$ where ρ , k_B , and T are the mean density, Boltzmann constant, and temperature. These observations of close-packed samples are in contrast, for example, with simple liquids for which $S(0) > 0$ [10]. The existence of hyperuniformity has been seen in a variety of systems, see for example discussions in Refs. [3, 11]. In general, long wavelength density fluctuations are important for diverse fields including critical phenomena [12] and the shear flow of glassy materials [13]. Likewise, understanding random close packed samples is relevant for understanding liquids, glasses, biological systems, and granular materials [1, 3, 14].

In 2010 we published an experimental study of a random close packed sample of colloidal particles, observed with confocal microscopy [15]. Our data set was the positions of more than 500 000 slightly polydisperse particles [16], and we found that $S(q \rightarrow 0) > 0$, implying that the experimental sample was compressible and not hyperuniform. A 2010 simulation of a binary sample found similar results [17]. These results seem to demonstrate random close packed samples that are not hyperuniform. However, in 2011 two groups showed that in polydisperse samples, careful consideration of the individual particle sizes recovers hyperuniformity and incompressibility [10, 11]. In particular, Berthier *et al.* showed how to compute the isothermal compressibility when the individual particle

sizes are known, and demonstrated that samples with $S(0) > 0$ nonetheless can be incompressible [10]. They examined data from a two-dimensional granular experiment and confirmed that $\chi(0) = 0$. The reason $S(0) > 0$ in polydisperse systems is because density fluctuations are coupled to composition fluctuations, but such samples can still be incompressible and hyperuniform.

In this article, we describe a method to determine each particle size from microscopy observations of a random close packed sample of colloidal particles. We use numerically generated packings to confirm that our method accurately determines the particle radii. Analyzing our experimental data using the method of Berthier *et al.* [10], we confirm that our experimental system is hyperuniform and incompressible. We additionally note an anticorrelation between the local polydispersity and local ordering.

As we use the analytical method introduced by Berthier *et al.* [10], we briefly summarize their method here. They consider a wave vector dependent isothermal compressibility $\chi(q)$ which is related to the structure factor of a *monodisperse* sample by $\rho k_B T \chi(q) = S(q)$. They then derive an exact formula relating $\chi(q)$ and $S(q)$ for a polydisperse sample, although the formula is “conceptually and computationally difficult” to evaluate [10]. Thus, they derive a series of approximate formulas, of which the first order approximation is sufficient for samples of low polydispersity such as ours. To start with, they define single-particle density fields $\rho_i(\mathbf{q}) = \exp(i\mathbf{q} \cdot \mathbf{r}_i)$ where \mathbf{r}_i is the position of particle i . They also define the size deviation of particle i as $\epsilon_i = (a_i - \bar{a})/\bar{a}$, where a_i is the radius of particle i and \bar{a} is the mean radius. (Note that $\sqrt{\langle \epsilon_i^2 \rangle} = p$ defines the polydispersity p of a sample.) These ϵ_i ’s are the small parameters used in the approximation. Using these variables, they define a 2×2 matrix $\mathbf{S}(q)$ with elements $S^{uv}(q) = \frac{1}{N} \langle \epsilon^u(\mathbf{q}) \epsilon^v(-\mathbf{q}) \rangle$, with $u, v \in 0, 1$, $\epsilon^u(q) = \sum_{i=1}^N \epsilon_i^u \rho_i(q)$, and N is the total number of particles. The matrix elements can be used to provide a first order approximation $\chi_1(q)$ as $\rho k_B T \chi_1(q) = S^{00} - [S^{01}]^2 / S^{11}$. They confirm that $\chi_1(0) \approx 0$ in cases for which the sample polydispersity is less than 10%, while $S(0) \neq 0$ for those cases.

Their results suggest that random close packed systems are hyperuniform and incompressible even when the sample is polydisperse [10].

In our prior work, we used colloidal particles to generate a random close packed sample, and imaged this with confocal microscopy. We reprise the key experimental points here; a more detailed experimental discussion is in Ref. [15]. We use sterically stabilized poly(methyl methacrylate) (PMMA) particles [18] with $\bar{a} = 1.265 \mu\text{m}$. Previously we reported that these particles had a polydispersity of $\sim 5\%$ [15]; below, we determine that the true polydispersity is 6.7%. The PMMA particles are suspended in a solvent mixture that is slightly lower density than the particles. The sample is mixed and then the particles are allowed to sediment until they are close packed. We use a confocal microscope to take clear images deep inside our dense sample [19]. Overlapping images are taken, with total volume $492 \times 514 \times 28 \mu\text{m}^3$. Within this volume, particles are identified within $0.03 \mu\text{m}$ in x and y , and within $0.05 \mu\text{m}$ in z [19, 21]. The total data set contains 543 136 particles [16].

The average particle size \bar{a} is obtained from the position of the first peak of the pair correlation function [15]. It is difficult to determine subtle size differences between individual particles from microscopy due to diffraction. However, obtaining the positions of each particle can be done fairly accurately. A large particle will be slightly farther from its neighbors as compared to a small particle, and we use this idea as a starting point for an estimation method for each particle size.

Given that our sample is jammed, each particle must be in contact with several of its neighbors. In fact, a numerical simulation of random close packed monodisperse particles showed that each particle contacts with at least 6 particles [20]. When particle i contacts with particle j , the separation between these two particles is given by $r_{ij} = a_i + a_j$, where a_i and a_j are their radii. The average of r_{ij} over all neighbors j is given by $\langle r_{ij} \rangle_j = a_i + \langle a_j \rangle_j$. Next, consider separations r_{jk} between particle i 's contacting neighbors j and contacting neighbors k of those particles. Again, we take an average of r_{jk} with respect to particles j and k , giving $\langle \langle r_{jk} \rangle_k \rangle_j = \langle a_j \rangle_j + \langle \langle a_k \rangle_k \rangle_j$. Then we subtract $\langle \langle r_{jk} \rangle_k \rangle_j$ from $\langle r_{ij} \rangle_j$, leading to

$$a_i = \langle \langle a_k \rangle_k \rangle_j + \langle r_{ij} \rangle_j - \langle \langle r_{jk} \rangle_k \rangle_j. \quad (1)$$

We choose the 5 nearest particles from particle i as the particles j , assumed to be in contact with particle i , and likewise for each particle j we identify its five closest neighbors for the particles k . For each particle j , one of its neighbors k should be particle i , leading to an overcounting in the average: $\langle \langle a_k \rangle_k \rangle_j = (1/5)a_i + (4/5)\langle \langle a_k \rangle_{k \neq i} \rangle_j$. Likewise, $\langle \langle r_{jk} \rangle_k \rangle_j = (1/5)\langle r_{ij} \rangle_j + (4/5)\langle \langle r_{jk} \rangle_{k \neq i} \rangle_j$ from the same overcounting of particle i . Using these results, we obtain

$$a_i = \langle \langle a_k \rangle_{k \neq i} \rangle_j + \langle r_{ij} \rangle_j - \langle \langle r_{jk} \rangle_{k \neq i} \rangle_j. \quad (2)$$

To compute $\langle \langle a_k \rangle_{k \neq i} \rangle_j$, we use \bar{a} as an initial guess for the particle sizes, and then iterate five times to get more

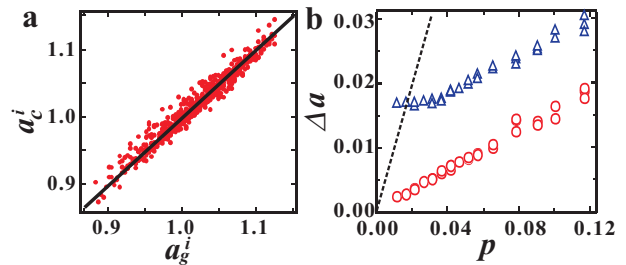


FIG. 1: (Color online) (a) Scatter plot of the calculated radius a_c^i from our method (Eqn. 2) as a function of the given radius a_g^i using data from a simulated packing with polydispersity 7%. The solid line corresponds to $a_c^i = a_g^i$. (b) The particle size uncertainty Δa found by analyzing simulation data from packings with a given polydispersity, both without noise (circles) and with noise added to the particle positions (triangles). The dashed line corresponds $\Delta a = p$.

accurate values for a_i . In this way a_i is found from the mean particle size and the particle separations, which are obtained directly from microscopy.

To validate our method, we simulate polydisperse rcp samples using the algorithm of Refs. [22, 23]. We use 512 particles with mean radius $\bar{a} = 1$ and polydispersity from 0.01 to 0.12, generating 5 independent configurations for each polydispersity. The particle size distribution is a Gaussian. Using the simulated position centers, we calculate the radii of the particles a_c^i by our method. Figure 1(a) shows a scatter plot of a_c^i as a function of the given radii a_g^i from a simulation with 7% polydispersity. The calculated radii are located around $a_c^i = a_g^i$. We define the uncertainty of the size estimation as $\Delta a = \sqrt{\langle (a_c^i - a_g^i)^2 / a_g^i \rangle_i}$. Δa is plotted as a function of polydispersity p as circles in Fig. 1(b). We find $\Delta a \approx p/6$. The polydispersity of a_c^i matches that of a_g^i .

One experimental complication is that there is an uncertainty in the position of each particle. In our experiment, the uncertainties are $0.024\bar{a}$ in x and y and $0.0395\bar{a}$ in z . We add this positional uncertainty to the true simulated positions, and then redetermine the particle radii. As expected, this increases the uncertainty Δa of the final radii, shown by the triangles in Fig. 1(b). Δa increases by ~ 0.01 compared to the case without positional noise. Positional noise is fatal when the polydispersity is less than 0.02, but otherwise our method results in more accurate radii even in the presence of noise.

Next, we estimate each particle size of our experimental data with our method. Given that Eqn. 2 requires information about both a particle's nearest neighbors and also second nearest neighbors, only particles sufficiently far from the edges of our images have accurate sizes. We modify our algorithm slightly for the experimental data as follows. We find the coordination number z_i of each particle, the number of neighboring particles within a distance $2.8a$ (the first minimum of the pair correlation function) [15]. From the particles in the interior

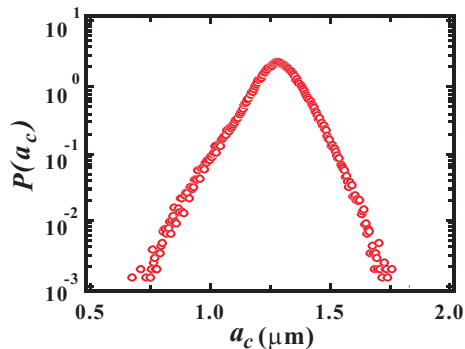


FIG. 2: (Color online) Probability of particle sizes in our experimental sample. The average size is $1.265 \mu\text{m}$ and polydispersity is 6.7%.

of the sample, we find the average coordination number $\bar{z} \approx 12$. Then, for every particle, we estimate the number of touching neighbors $T_i = 5z_i/12$ where we round T_i to the nearest integer. For particles at the edge of the imaged volume, $T_i < 5$ as not all of the neighbors are imaged. Then for each particle, when averages over contacting neighbors j are done in Eqn. 2, these averages are over the T_i nearest neighbors. After iterating Eqn. 2 to find all radii, the edge particles are removed by cropping the data to a volume of $440 \times 461 \times 14.2 \mu\text{m}^3$, containing 217 816 particles.

Based on these particles with their calculated sizes, the volume fraction of this sample is found to be $\phi = 0.647 \pm 0.007$, where the uncertainty of ϕ is due to the uncertainty in determination of each particle size. Figure 2 shows a distribution of the estimated particle sizes. This sample has a polydispersity of 6.7%. Given this measured polydispersity, Fig. 1(b) shows that $\Delta a \approx 0.023$ (corresponding to $\bar{a}\Delta a = 0.03 \mu\text{m}$). The experimental distribution is not a Gaussian and this is not an artifact of our method, as a simulated Gaussian size distribution with positional noise leads to a measured Gaussian size distribution.

Using our estimated particle sizes, we now study the wave vector dependence of the compressibility $\chi_0(q)$ and $\chi_1(q)$ of our experimental data. Figure 3 shows $\rho k_B T \chi_0(q)$ and $\rho k_B T \chi_1(q)$. Our experimental data do not obey periodic boundary conditions, and the effect of the boundaries appears near $q = 0$. $\chi_0(q)$ and $\chi_1(q)$ are independent of the choice of Fourier window functions for $q\bar{a}/\pi > 0.2$. Thus we do a linear fit to $\rho k_B T \chi_0(q)$ and $\rho k_B T \chi_1(q)$ in the region $0.2 < q\bar{a}/\pi < 0.5$, shown as the lines in Fig. 3; both functions have linear behavior in this region. We find $\rho k_B T \chi_1(0) = 0.002 \pm 0.004$, while $\rho k_B T \chi_0(0) = 0.049 \pm 0.008$ as reported previously [15]. The uncertainties are due to the uncertainties of particle positions and sizes, and the choice of the fitting range. Our observation that $\chi_1(q) \sim q$ shows that long wavelength density fluctuations are suppressed. This is consistent with the observations of Berthier *et al.* and

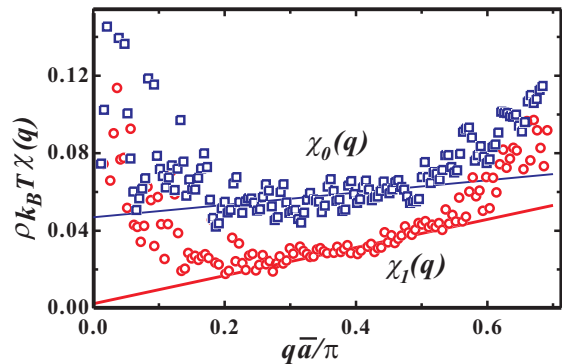


FIG. 3: (Color online) $\rho k_B T \chi_0(q)$ (no approximation) and $\rho k_B T \chi_1(q)$ (first order approximation of Ref. [10]), from the experimental data. Square symbols correspond to $\rho k_B T \chi_0(q)$, which is proportional to $S(q)$ at small q . Circle symbols correspond to $\rho k_B T \chi_1(q)$. The lines are linear fits to the data for $0.2 < q\bar{a}/\pi < 0.5$.

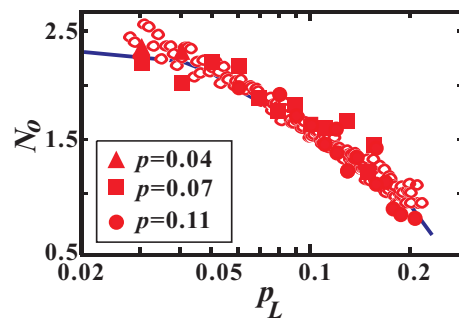


FIG. 4: (Color online) The number of ordered neighbors N_o as a function of the local polydispersity p_L in the experiment (open circles) and simulations (bulk polydispersities as indicated in legend). The line is the average of N_o from 75 simulated systems with bulk polydispersity from 1% to 12%.

show that our system is incompressible and likely hyperuniform [10].

Our data let us consider a new question, the relationship between local environment and local ordering. It is known that crystallization occurs in samples with low polydispersity ($p < 0.08$) [24–26]. However, crystal nucleation is a microscopic phenomenon, that is, the crystal nuclei do not necessarily “know” the bulk polydispersity. We can use our data to investigate the relationship between local ordering and local polydispersity.

We define the local polydispersity p_L^i as

$$p_L^i = \sqrt{\langle (a_n - a_i)^2 \rangle} / a_i \quad (3)$$

where $\langle a_n \rangle$ is the mean radius of the nearest neighbor particles of particle i . The nearest neighbors of a particle are defined as those with centers separated by less than $2.8a$ [15]. We calculate the bond order parameter d_6^{in} to quantify how the local structure compares between neighbors i and n [27–29]. Two neighboring particles are termed

“ordered neighbors” if d_6^{in} exceeds a threshold value of 0.5 [27–29]. We then count the number of ordered neighbors N_o^i around each particle i . $N_o^i = 0$ corresponds to random structure around particle i , while $N_o^i > 7$ means that particle i is in a crystalline environment [29].

Figure 4 shows that the local polydispersity p_L^i has a strong influence on local order N_o^i . The open circles show the result from our experiment. Particles with low p_L are more ordered than particles with high p_L : that is, there is a tendency for particles to order when the central particle size a_i is similar to its surrounding neighbors. A similar result is found from our simulated packings (closed symbols and solid line in Fig. 4), where the local polydispersity predicts local order independent of the global polydispersity. The agreement between the simulations and the experiment is striking, especially given that the simulation corresponds to an extremely fast quench, whereas the experimental quench allows time for particles to rearrange [15]. Note that these conclusions are unchanged when a_i in Eqn. 3 is replaced by $\langle a_n \rangle$, although the trend shown in Fig. 4 is less pronounced. Our results are consistent with the prior knowledge that polydispersity affects the ability to crystallize [24–26], but this is the first examination we are aware of showing how polydispersity can have a local influence on crystallization. It suggests an intuitively reasonable idea, that in a moderately polydisperse sample, crystalline nuclei are more likely to form from locally monodisperse patches.

We note that the observed polydispersity of our sample (6.7%) helps explain a discrepancy we noted between our observations [15] and those of Dullens *et al.*, who also studied dense suspensions of sedimenting particles with similar sedimentation rates [30]. They observed that particles formed crystals in all cases [30], while our particles pack randomly. Their samples had a polydispersity of 5%, while our sample is 6.7%. Crystal nucleation is sensitive to polydispersity in this range [26] and this likely explains why our sample avoids crystallization, and why the samples of Dullens *et al.* crystallized.

To summarize, we have presented a method to estimate the sizes of individual colloidal particles from experimental knowledge of only their positions, and relying on the fact that the sample is close-packed. Numerical simulations confirm that our method is robust even in the presence of realistic experimental noise. Using the positions and sizes of over 200 000 random close packed particles from our experiment, we confirm that our experimental system is hyperuniform and incompressible. Our results are consistent with prior work [10] and the data can be used with other algorithms for quantifying hyperuniformity in polydisperse samples [11]. We also see a relationship between local polydispersity and local order, confirming that locally a higher polydispersity results in less ordered packing.

E. R. W. was supported by a grant from the National Science Foundation (CHE-0910707).

-
- [1] W. O. Smith, P. D. Foote, and P. F. Busang, *Phys. Rev.* **34** 1271 (1929).
 - [2] A. E. R. Westman and H. R. Hugill, *J. Am. Ceram. Soc.* **13**, 767 (1930).
 - [3] S. Torquato and F. H. Stillinger, *Rev. Mod. Phys.* **82**, 2633 (2010).
 - [4] S. Torquato, T. M. Truskett and P. G. Debenedetti, *Phys. Rev. Lett.* **84**, 2064 (2000).
 - [5] M. Clusel, E. I. Corwin, A. O. N. Siemens, and J. Brujic, *Nature* **460**, 611 (2009).
 - [6] A. Donev *et al.*, *Science* **303**, 990 (2004).
 - [7] E. Chen, M. Engel, and S. Glotzer, *Discrete & Comp. Geom.* **44**, 253 (2010).
 - [8] A. Donev, F. H. Stillinger and S. Torquato, *Phys. Rev. Lett.* **95**, 090604 (2005).
 - [9] L. E. Silbert and M. Silbert, *Phys. Rev. E* **80**, 041304 (2009).
 - [10] L. Berthier, P. Chaudhuri, C. Coulais, O. Dauchot and P. Sollich, *Phys. Rev. Lett.* **106**, 120601 (2011).
 - [11] C. E. Zachary, Y. Jiao, and S. Torquato *Phys. Rev. Lett.* **106**, 178001 (2011); *Phys. Rev. E* **83**, 051308 (2011); *Phys. Rev. E* **83**, 051309 (2011).
 - [12] A. Onuki, *Phase Transition Dynamics* (Cambridge University Press, Cambridge, England, 2002).
 - [13] A. Furukawa and H. Tanaka, *Nature Mater.* **8**, 601 (2009).
 - [14] J. D. Bernal and J. Mason, *Nature* **188**, 910 (1960).
 - [15] R. Kurita and E. R. Weeks, *Phys. Rev. E* **82**, 011403 (2010).
 - [16] A file of the particle coordinates is available at <http://link.aps.org/supplemental/10.1103/PhysRevE.82.011403>
 - [17] N. Xu and E. S. C. Ching, *Soft Matter* **6**, 2944 (2010).
 - [18] L. Antl *et al.*, *Colloid Surf.* **17**, 67 (1986).
 - [19] A. D. Dinsmore, E. R. Weeks, V. Prasad, A. C. Levitt, and D. A. Weitz, *Appl. Opt.* **40**, 4152 (2001).
 - [20] S. Torquato and F. H. Stillinger, *Phys. Rev. E* **68**, 041113 (2003). **68**, 069901 (2003).
 - [21] J. C. Crocker and D. G. Grier, *J. Colloid Interface Sci.* **179**, 298 (1996).
 - [22] N. Xu, J. Blawdziewicz, and C. S. O’Hern, *Phys. Rev. E* **71**, 061306 (2005).
 - [23] K. W. Desmond and E. R. Weeks, *Phys. Rev. E* **80**, 051305 (2009).
 - [24] H. J. Schope, G. Bryant and W. van Meegen, *J. Chem. Phys.*, **127**, 084505 (2007).
 - [25] S. I. Henderson and W. van Meegen, *Phys. Rev. Lett.*, **80**, 877 (1998).
 - [26] S. Auer and D. Frenkel, *Nature* **413**, 711 (2001).
 - [27] P. J. Steinhardt, D. R. Nelson and M. Ronchetti, *Phys. Rev. B* **28**, 784 (1983).
 - [28] U. Gasser, E. R. Weeks, A. Schofield, P. N. Pusey, and D. A. Weitz, *Science* **292**, 258 (2001).
 - [29] P. Rein ten Wolde, M. J. Ruiz-Montero, and D. Frenkel, *J. Chem. Phys.* **104**, 9932 (1996).
 - [30] R. P. A. Dullens, D. G. A. L. Aarts and W. K. Kegels, *Phys. Rev. Lett.* **97**, 228301 (2006).